Direct Search Algorithm for Load Frequency Control of a Time-Delayed Electric Vehicle Aggregator

Roozbeh Abolpour, Khashayar Torabi, Maryam Dehghani, *Senior Member, IEEE,* Navid Vafamand, Mohammad S. Javadi, *Senior Member, IEEE*, Fei Wang, *Senior Member, IEEE*, João P. S. Catalão, *Fellow, IEEE*

***Abstract*—This paper addresses the topic of frequency regulation of a single-area power system connected to an electric vehicle (EV) aggregator over a non-ideal communication network. It is considered that the command control action is received by the EV aggregator with constant delay and the power system includes uncertain parameters. Due to the presence of uncertainties and the delay term, the frequency regulation problem is non-convex and hard to solve. The present approaches in the literature convert the non-convex control design problem into a convex problem with a set of Linear Matrix Inequalities (LMIs), which is conservative and in many cases results infeasibility. In this paper, an innovative iterative algorithm, called direct search, is employed for the time-delayed system to design the unknown parameters of a pre-assumed controller. The controller choice is not limited and various controllers' structures can be assumed. Without loss of generality, a proportional-integral (PI) controller is designed. The novel direct search algorithm can determine a feasible solution whenever at least one solution lays in the design space. Hence, by selecting a wide design space, we can anticipate that the PI controller guarantees closed-loop stability. Numerical simulations are carried out to demonstrate the performance of the developed controller compared to the state-of-the-art approach.**

***Index Terms*—Load frequency control, electric vehicle aggregator, Lyapunov Krasovskii Functional (LKF), robust control, direct search algorithm, time delay.**

I. Introduction

A. *Motivation and background*

Load frequency control (LFC) is a key issue in power systems [1], which are vulnerable to the inconsistency of consuming and generating electrical power, specially the systems including several renewable energy sources.

Emerging renewable and pollution-free sources offer the merit of reducing the environmental pollution and demerit of degrading power quality [2]. In this regard, the role of batteries and fast response generators is becoming increasingly important. On the other hand, emerging electric vehicles (EVs) and vehicle-to-grid (V2G) technology is a promising solution dealing with the degrading influence of renewable energy sources on the LFC system. EVs' batteries are classified as fast response elements in the LFC system. In comparison to conventional generators, by operating as both loads or generators, the EV batteries regulate the electric power of AC grids remarkably faster and enhance the dynamic performance of the LFC system [3].

Instead of connecting each of the EV units, EV aggregators are required. As their name suggests, they aggregate and control several EVs, which are available in the parking lots. The EV aggregators communicate with the power system and the LFC center by sending their status of available battery capacities and electric power, receiving the control commands to regulate the charging and discharging actions of the EVs [4].

From a practical point of view, the EV aggregators use a communication network with low cost and bandwidth to transfer data. Therefore, the communication link is vulnerable to delays and missing data [5],[6]. These issues adversely affect LFC system performance and stability [7]. Hence, this paper studies the LFC of EV aggregators in the presence of delay via a less-conservative approach compared to the present ones.

B. *Literature review*

The stability analysis for multi-area LFC systems in the presence of EVs, and taking into consideration time delays, has been addressed in [8], where the partial integral equation was utilized for the LFC system modeling with EVs, and afterward, a thorough quadratic LKF was formed as an inner product of the linear partial integral operator.

Ref. [9] utilized a discrete LFC system with a fast response, which is directly developed using the sampled-data control and applied to a wind energy integrated power system. A discrete-time approach was used in [10] for analyzing an LFC system associated with sampled data and time delay in the presence of prevalent generating units and storage systems. In this respect, a matrix uncertainty technique was employed to characterize the impact of time-varying delays.

Ref. [11] developed a cooperative LFC system for a multi-area power system being capable of successfully tackling the coordination issue of the LFC systems. A supplementary LFC mechanism has been introduced in [12] employing EVs and heat pump water heaters in the presence of a high penetration level of wind and solar power generation.

Corresponding authors: F. Wang and J.P.S. Catalão.

R. Abolpour, K. Torabi, M. Dehghani and N. Vafamand are with School of Electrical and Computer Engineering, Shiraz University, Shiraz, Iran (e-mails: {r.abolpour, kh.torabi, mdehghani, vafamand}@shirazu.ac.ir).

M.S. Javadi is with the Institute for Systems and Computer Engineering Technology and Science (INESC TEC), Porto, Portugal (e-mail: msjavadi@gmail.com).

F. Wang is with the Department of Electrical Engineering, North China Electric Power University (NCEPU), Baoding 071003, China, also with the State Key Laboratory of Alternate Electrical Power System with Renewable Energy Sources (NCEPU), Beijing 102206, China, and also with the Hebei Key Laboratory of Distributed Energy Storage and Microgrid (NCEPU), Baoding 071003, China (e-mail: feiwang@ncepu.edu.cn).

J.P.S. Catalão is with the Faculty of Engineering of the University of Porto (FEUP) and INESC TEC, Porto 4200-465, Portugal (e-mail: catalao@fe.up.pt).

To tackle the robust stability of LFC systems, advanced control techniques emerged, some of them are sliding mode [13], event-triggered [14], and μ-syntheis [2] approaches. The stability of an event-triggered LFC of time-delayed single-area and multi-area power systems has been addressed in [15], where the stability index is less conservative. In this respect, the delay-dependent stability condition is enhanced using a lifting method and a two-side looped Lyapunov functional. An event-triggered LFC system has been developed in [16] for a time-delayed power system to ensure the stability and H_∞ index of the closed-loop system under deception attacks.

A combined H_2/H_∞ has been developed in [17] for the LFC using the V2G capability of EVs to deal with time-varying load demand and volatile renewable power generation, besides the deadbands and time delays relating to the controller itself and EV aggregators. An adaptive fractional-order fuzzy PID controller has been designed in [18] for the LFC of an islanded renewable energies-penetrated microgrid. The proposed controller has been enhanced by embedding a metaheuristic optimization algorithm to tune the parameters. In this relation, the V2G capability of EVs was suggested to be employed.

A sliding mode control mechanism was introduced in [19] for the LFC system of a multi-area power system, where a hybrid energy storage system was deployed to promote the LFC system. It was shown that the proposed framework could effectively handle the fluctuations occurring in the frequency and tie-line power due to load disturbances. Ref. [20] proposed a model-free control scheme using the sliding mode control for the secondary LFC of a time-delayed islanded microgrid in the presence of EVs. The proposed controller's performance was fortified by applying a metaheuristic optimization algorithm named "the black hole method". Ref. [21] developed a high-order sliding mode control for a multi-area LFC system in the presence of non-linear sources.

A distributed observer-based control scheme has been designed in [22] for the LFC of a multi-area power system interconnected through high-voltage direct current (HVDC) lines. In this regard, every area of the system was equipped with a controller and the fleets of EVs were supposed to assist thermal units in facing stability issues arising from the varying load demand. The superior performance of the presented scheme was verified through a comparison made with the centralized observer-based controller for the mentioned system.

More recently, the LFC issue under communication delay [3], [23]–[26] received much attention. An enhanced integral derivative-tilted control scheme has been designed in [27] for the LFC system of a multi-area power system taking into account various energy resources, both renewable and non-renewable, and communication time delays, besides the governor deadband and other constraints.

In [23], a proportional integral derivative (PID) was suggested for time-delayed LFC, and sufficient controller design conditions were re-formulated in terms of linear matrix inequality (LMI) constraints. In [24], a predictive method was suggested based on state-feedback to regulate the frequency in the presence of time-delayed control input. The controller design conditions are stated in terms of LMIs.

A model predictive control-based scheme has been suggested in [28] for the LFC system of a distribution network with four energy hubs. In this respect, the fleets of EVs and home appliances as responsive loads have been used for the LFC. Ref. [29] suggested a distributed model predictive control scheme for a multi-area LFC system. The mentioned controller was based on the cooperation distributed economic scheme where the asymptotic stability was verified.

A differential game-based cooperative control strategy was developed in [30] for the multi-area LFC system, where a more desired regulation capacity allocation was achieved compared to the prevalent PI and optimal control mechanisms.

In [25], based on the Lyapunov stability theory and LMI, the stability delay margin of an LFC system was analyzed. The stability of multi-area LFC systems with EV aggregators and time delays has been studied in [25] using the LKF approach. To this end, two stability indices were obtained by employing the Bessel-Legendre inequality and model reconstruction method. The delay-dependent stability analysis has been carried out in [31] using the closed-loop models for a single-area LFC system in the presence of EVs, while the LKF technique was applied to propose two delay-dependent stability indices.

In [26], the stability delay margin was investigated based on the frequency response of a LFC system by deploying a frequency sweeping test and the binary iteration algorithm. In [3], the stability analysis is performed based on the stability boundary locus. The effect of time-delay and control command participation on the PI controller gains was studied. In [32], a graphical method to compute stabilizing PI values is provided.

Although such advanced control methods were successful in satisfying the desired performances, the computational burden and conservativeness of such techniques have been reported as their common drawbacks. Also, the effect of system uncertainties on the closed-loop time delayed LFC has not been studied, yet.

C. *Paper contribution*

This paper deals with the load frequency control (LFC) of single-area power system connected to an electric vehicle. For the uncertain time-delayed EV aggregator model, a robust PI controller is devised, being resilient against system uncertainties and time delays. The proposed approach for frequency regulation is based on the idea of direct searching. This idea generally consists of two methods, one for detecting the stabilizing point and one for detecting the undesired parts of the design space. The algorithm iteratively searches a given design space through a branch-and-bound technique whose strategies are based on omitting the undesired parts of the design space and checking the feasibility of some special points. The proposed algorithm is mathematically proved to have important performances including finite termination and feasibility convergence, for the first time. In fact, the proposed algorithm is able to find a stabilizer point for the mentioned system; however, the other existing methods do not guarantee the equivalent feasibility situation since they convert the non-convex control design problem into a convex problem with a set of LMI conditions which is certainly not equivalent to the original problem. Finite termination and non-conservativeness are two major novelties of the proposed algorithm over the existing design controller methods.

To show the merits of the suggested method, comprehensive numerical simulations are conducted and the effect of system

parameters and time delay value on the closed-loop stability margin and controller gains are studied. Finally, the results are compared with the existing approach.

D. *Paper structure*

This paper is continued as follows: In Section II, the LFC problem with EV aggregator and time delay is presented. In Section III, the proposed direct search algorithm to design the frequency controller is discussed. In this section, the existing approach based on LKF is presented. Then, the direct search approach for the LFC stabilization is presented. In Section IV, comprehensive simulations in various scenarios, in presence of time-varying delays, uncertainties and disturbances are conducted. Section V ends this paper by evoking some concluding remarks and future perspectives.

II. SINGLE-AREA LFC SYSTEM MODEL WITH EV AGGREGATOR

EV aggregator units facilitate frequency regulation for EVs in parking lots. The EV aggregators are connected to control centers and receive the controller commands to inject or absorb electric power and allocate it among each of the participating EVs. To investigate the stability of the power system, a single-area LFC system connected to an EV aggregator is considered. The schematic of a typical single-area LFC system including a generator, an EV aggregator, delay block, and the droop and PI controllers is drawn in Fig. 1. As can be seen in Fig. 1, Δf is the deviation of power system frequency. ΔP_g, ΔP_{EV}, and ΔP_d are electrical output power, EV aggregator output power, and load disturbance, respectively.

The sum of the powers will affect the power system frequency. ΔX_g and ΔP_m are the valve position and mechanical output power, respectively. Furthermore, D and M are the damping coefficient and generator inertia constant, R is the speed droop, F_p, T_g, T_r, and T_c are the fraction of the total turbine power, the time constant of the governor, reheat and turbine, respectively, β is the frequency bias factor, and α_0 and α_1 are the participation factors.

The PI controller gains are K_p and K_I. The control signal is fragmented among the generator and the EV by α_0 and α_1 and transmitted to the EV through the communication networks with the delay τ. As can be seen in Fig. 1, a communication delay between the controller and the generator is not considered, because it is ignorable compared to the EV link.

The objective is to choose PI controller gains $F = [K_p, K_I]^T$ for regulating the frequency. This issue is influenced by the communication delay τ and the participation factor vector $\alpha = [\alpha_0, \alpha_1]^T$. If these parameters are not involved in the design procedure, the overall stability will be compromised.

It should be noted that the participation factors and the communication delay are supposed to be uncertain parameters. The region of these parameters should be determined at the beginning. The participation factors' region is denoted by $\Omega = [0.7,1] \times [0,0.3]$ in this paper and the delay parameter is considered to belong to $[0, \bar{\tau}]$, in which $\bar{\tau}$ is a given known parameter. Based on Fig. 1, the characteristic equation can be written as follows:

$$q(s, F, \alpha, \tau) = P(s, F, \alpha) + W(s, F, \alpha)e^{-\tau s} \tag{1}$$

where $P(.)$ and $W(.)$ are polynomials with real coefficients in terms of system parameters, as follows:

$$P(.) = p_6 s^6 + p_5 s^5 + p_4 s^4 + p_3 s^3 + p_2 s^2 + p_1 s^1 + p_0 \tag{2}$$

$$W(.) = w_4 s^4 + w_3 s^3 + w_2 s^2 + w_1 s^1 + w_0 \tag{3}$$

$$\begin{cases} p_6 = MRT_gT_rT_cT_{EV} \\ p_5 = DRT_gT_rT_cT_{EV} + MR(T_g T_rT_c + T_rT_cT_{EV} \\ +T_gT_cT_{EV} + T_gT_rT_{EV} \\ p_4 = DR\left(T_gT_rT_c + T_rT_cT_{EV} + T_gT_cT_{EV} + T_gT_rT_{EV}\right) \\ +MR\left(T_rT_c + T_gT_c + T_gT_r + T_cT_{EV} + T_rT_{EV} + T_gT_{EV}\right) \\ p_3 = F_PT_rT_{EV} + \alpha_0\beta RK_pF_PT_rT_{EV} \\ +MR\left(T_c + T_r + T_g + T_{EV}\right) \\ +DR\left(T_rT_c + T_gT_c + T_gT_r + T_cT_{EV} + T_rT_{EV} + T_gT_{EV}\right) \\ p_2 = DR\left(T_c + T_r + T_g + T_{EV}\right) + MR + F_PT_r \\ +T_{EV} + \alpha_0\beta R\left(K_pT_{EV} + K_pF_PT_r + K_IF_PT_rT_{EV}\right) \\ p_1 = DR + 1 + \alpha_0\beta R\left(K_p + K_IT_{EV} + K_IF_PT_r\right) \\ p_0 = \alpha_0\beta RK_I \end{cases} \tag{4}$$

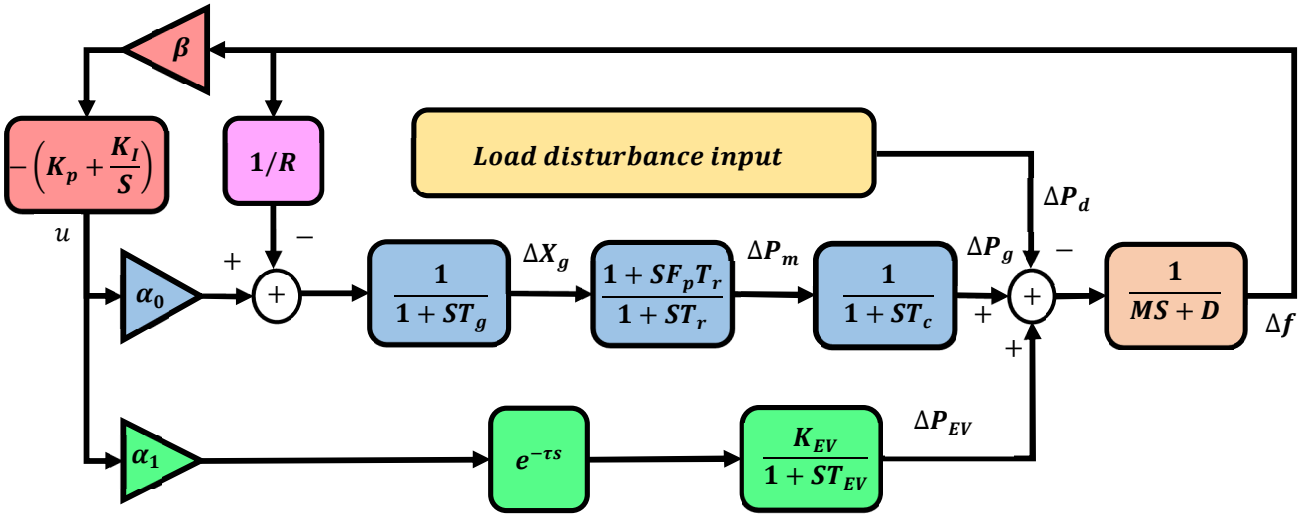

Fig. 1. The schematic of a single area LFC system.

$$\begin{cases} w_4 = \alpha_1\,\beta R K_{EV} K_P T_g T_r T_c \\ w_3 = \alpha_1\,\beta R K_{EV}(K_P T_r T_c + K_P T_g T_c \\ \qquad +K_P T_g T_r + K_I T_g T_r T_c) \\ w_2 = \alpha_1\,\beta R K_{EV}(K_P T_c + K_P T_r + K_P T_g \\ \qquad +K_I T_r T_c T_c + K_I T_g + K_I T_g T_r) \\ w_1 = \alpha_1\,\beta R K_{EV}\left(K_P + K_I T_c + K_I T_r + K_I T_g\right) \\ w_0 = \alpha_1\,\beta R K_{EV} K_I \end{cases} \quad (5)$$

The LFC power system parameters are given in Table I. Using $z = e^{-\tau s}$, the characteristic equation can be written as $\hat{q}(s, F, \alpha, z) = P(s, F, \alpha) + W(s, F, \alpha)z$. This characteristic polynomial is a two-variate polynomial that is a function of both s and z. In the next section, an algorithm is proposed that can design the controller parameters for the two-variate polynomial.

TABLE I: EV AGGREGATORS' NOMINAL VALUES WITH UNCERTAINTY BOUNDS

Parameter	Value	Parameter	Value
T_g	0.2 s	R	1.11 $Hz/p.u.MW$
T_c	0.3 s	K_{EV}	1 s
T_r	12 s	M	8.8
T_{EV}	0.1 s	D	1
F_P	1.6	α_0	$\in$ [0.7 1]
β	21	α_1	$\in$ [0 0.3]

III. PROPOSED APPROACH FOR EV STABILIZATION EVALUATION

In this section, the proposed direct search approach for the EV stabilization evaluation is presented. The direct search idea considers a solution space (primary design space) for the unknown controller parameters and includes two methods, one for detecting the stabilizing point (given in subsections A and B), and one for detecting the undesired parts of the design space (given in subsection C). Based on the theories for detecting a stabilizing point and undesired points, the algorithm systematically and iteratively considers sub-spaces within the design space, checks the stability status of the corner points of the considered sub-space and the whole space, and decides whether the whole sub-space is undesired which should be omitted from the design space instantly, or a feasible point is found in one of the corners which is surely the solution. By checking various sub-spaces in the whole design space, we will be able to be assured about the closed-loop stability of the design space points in the presence of system uncertainties and time delay terms.

Also, in this section we prove that the proposed algorithm has important performances including finite termination (proved by Theorem 4) and feasibility convergence (proved by Theorem 5) for the first time. In fact, compared to the other existing methods that do not guarantee the equivalent feasibility situation because they approximate the overall non-convex problem with a set of LMI conditions, the proposed approach presents a non-conservative methodology for solving the controller design problem of the uncertain time-delay system in section II.

A. *Lyapunov Krasovskii Functional based design algorithm*

This subsection presents a method to find an appropriate design vector that stabilizes the LFC power system through a Lyapunov Krasovskii idea. Firstly, Theorem 1 proposes a set of conditions to assess the stability of the closed loop LFC power system for a given design point. The proposed conditions are not entirely convex due to the existence of coupling terms between the design and Lyapunov parameters. Secondly, an algorithm is presented to solve the conditions of Theorem 1 through grouping the free variables in two separate steps in each iteration to decouple the bilinear terms in these conditions and solve the LKF approach through LMIs.

Theorem 1 [33]. *The given design point* $F = [K_P \quad K_I]^T$ *asymptotically stabilizes the LFC system if there exist positive definite matrices* $P = \begin{bmatrix} P_{11} & P_{12} & P_{13} \\ * & P_{22} & P_{23} \\ * & * & P_{33} \end{bmatrix}$, Q_1, Q_2, Q_3, R_1, R_2, U_1, *and* U_2 *and also matrices* T_1, T_2, T_3, Y_1, Y_2, *and* Y_3 *with appropriate dimensions such that they hold the following LMIs for* $\tau \in \{0, \bar{\tau}\}$ *and* $\alpha \in \partial_c(\Omega)$

$$\forall i \in \{1,2,\dots,N\}: \begin{bmatrix} E_i & A_c(F,\alpha)^T S_i & \frac{\bar{\tau}}{N} Y \\ * & -S_i & 0 \\ * & * & -\frac{\bar{\tau}}{N} R_2 \end{bmatrix} \le 0 \quad (6)$$

$$\forall i \in \{1,2,\dots,N\}: \begin{bmatrix} E_i & A_c(F,\alpha)^T S_i & \frac{\bar{\tau}}{N} T \\ * & -S_i & 0 \\ * & * & -\frac{\bar{\tau}}{N} R_2 \end{bmatrix} \le 0 \quad (7)$$

where some of the above matrices are defined here:

$$E_i = \begin{bmatrix} E_{i_{11}} & E_{i_{12}} & E_{i_{13}} & E_{i_{14}} & E_{i_{15}} & E_{i_{16}} \\ * & E_{i_{22}} & E_{i_{23}} & E_{i_{24}} & E_{i_{25}} & E_{i_{26}} \\ * & * & E_{i_{33}} & E_{i_{34}} & E_{i_{35}} & E_{i_{36}} \\ * & * & * & E_{i_{44}} & E_{i_{45}} & E_{i_{46}} \\ * & * & * & * & E_{i_{55}} & E_{i_{56}} \\ * & * & * & * & * & E_{i_{66}} \end{bmatrix} \quad (8)$$

$$E_{i_{11}} = sym(P_{11}A(F.\alpha) + P_{12}) + Q_1 + Q_2 + Q_3 - \tau_i^2 U_1 - \left(\frac{\bar{\tau}}{N}\right)^2 U_2 \quad (9)$$

$$E_{i_{12}} = -P_{12} + P_{13}, E_{i_{13}} = P_{11}A_d(F.\alpha), E_{i_{14}} = -P_{13} \quad (10)$$

$$E_{i_{15}} = A(F.\alpha)^T P_{12} + P_{22} + \tau_i U_1 \quad (11)$$

$$E_{i_{16}} = A(F.\alpha)^T P_{13} + P_{23} + \frac{\bar{\tau}}{N} U_2 \quad (12)$$

$$E_{i_{22}} = -Q_1 - 2R_1 + Y_1 + Y_1^T, E_{i_{23}} = -Y_1 + T_1 + Y_2^T \quad (13)$$

$$E_{i_{24}} = -T_1 + Y_3^T, E_{i_{25}} = -P_{22} + P_{23}^T + \frac{2}{\tau_i} R_1 \quad (14)$$

$$E_{i_{26}} = -P_{23} + P_{33} \quad (15)$$

$$E_{i_{33}} = -Q_3 + sym(T_2 - Y_2), E_{i_{34}} = T_3^T - T_2 - Y_3^T \quad (16)$$

$$E_{i_{35}} = A_d(F.\alpha)^T P_{12}, E_{i_{36}} = A_d^T P_{13} \quad (17)$$

$$E_{i_{44}} = -T_3 - T_3^T - Q_2, E_{i_{45}} = -P_{23}^T, E_{i_{46}} = -P_{33} \quad (18)$$

$$E_{i_{55}} = -U_1 - \frac{2}{\tau_i^2} R_1, E_{i_{56}} = 0, E_{i_{66}} = -U_2 \quad (19)$$

$$A(F.\alpha) = \begin{bmatrix} 0 & 1 & 0 & 0 & 0 & 0 \\ 0 & 0 & 1 & 0 & 0 & 0 \\ 0 & 0 & 0 & 1 & 0 & 0 \\ 0 & 0 & 0 & 0 & 1 & 0 \\ 0 & 0 & 0 & 0 & 0 & 1 \\ -\frac{p_0}{p_6} & -\frac{p_1}{p_6} & -\frac{p_2}{p_6} & -\frac{p_3}{p_6} & -\frac{p_4}{p_6} & -\frac{p_5}{p_6} \end{bmatrix} \quad (20)$$

$$A_d(F,\alpha) = \begin{bmatrix} 0 & 0 & 0 & 0 & 0 & 0 \\ 0 & 0 & 0 & 0 & 0 & 0 \\ 0 & 0 & 0 & 0 & 0 & 0 \\ 0 & 0 & 0 & 0 & 0 & 0 \\ 0 & 0 & 0 & 0 & 0 & 0 \\ -\frac{w_0}{p_6} & -\frac{w_1}{p_6} & -\frac{w_2}{p_6} & -\frac{w_3}{p_6} & -\frac{w_4}{p_6} & 0 \end{bmatrix} \quad (21)$$

$$S_i = \tau_i^2 R_1 + \frac{\bar{\tau}}{N} R_2 + \frac{1}{4}\tau_i^4 U_1 + \frac{1}{2}(\tau_{i+1}^2 - \tau_i^2) U_2 \quad (22)$$

$$A_c(F,\alpha) = [A(F,\alpha) \quad 0 \quad A_d(F,\alpha) \quad 0 \quad 0 \quad 0] \quad (23)$$

$$Y = [0 \quad Y_1^T \quad Y_2^T \quad Y_3^T \quad 0 \quad 0] \quad (24)$$

$$T = [0 \quad T_1^T \quad T_2^T \quad T_3^T \quad 0 \quad 0] \quad (25)$$

where $\partial_c(\Omega)$ contains the corner points of the design space for α_0 and α_1, N is a given number, Ω is the considered uncertain space.

Remark 1. *It should be noted that the conditions of Theorem 1 given in (6-7) cannot be directly solved considering the design vector F contains free variables. It is mainly because these conditions are not affine functions of the free variables which means they are not LMI. The crossing terms between unknown variables make them Bilinear Matrix Inequalities (BMIs).*

To solve (6-7), the P-K design algorithm is exploited based on Theorem 1. The algorithm trees to solve the conditions in consecutive iterations such that two steps are performed in each iteration. In the first step, conditions (6-7) are solved under the assumption of the design vector F is fixed and known to obtain the Lyapunov variables. In the second step, conditions (6-7) are solved for known Lyapunov parameters to achieve the control variables in F. These steps are repeated in each iteration and the algorithm continues to reach a feasible solution.

It should be noted that the above iterative algorithm does not guarantee convergence to a feasible point. Obviously, we may encounter some cases where a stabilizing point exists, but the algorithm cannot find the solution. To overcome this problem, an equivalent stabilization condition is proposed in the next sub-section. The algorithm can guarantee finding a feasible point if it exists.

B. *Equivalent stabilization condition for LFC system*

The main idea of this section is to directly search a primary design space through an iterative algorithm. The design space is divided to some simplexes. Then, one is considered as the active simplex and the algorithm checks its stability status. If it is completely infeasible which assures no feasible point is inside the simplex, it is deleted from the design space and the algorithm continues its search in the remained parts of the design space.

Assume that we have a primary design space as the boundary of the area shown in Fig. 2. In the literature, there are some heuristic approaches such as Genetic Algorithm (GA) or Particle Swarm Optimization (PSO) that search the design space for a stabilizing solution. However, they do not have any convergence proof. Our algorithm does surely have a convergence proof. The idea is to divide the design space into some simplexes. Then, check the stability status of the corner points of the simplex. Through them, we can understand whether the whole simplex is infeasible or not. If the simplex is infeasible, it is omitted. If one of the corner points is a stabilizing point, it is the solution and the algorithm stops. Otherwise, the simplex should be divided to two smaller ones and the search continues in the new-generated simplexes. A sample design space is shown in Fig. 2. The colored simplexes are surely infeasible and they are omitted. The white ones are still needed to be searched.

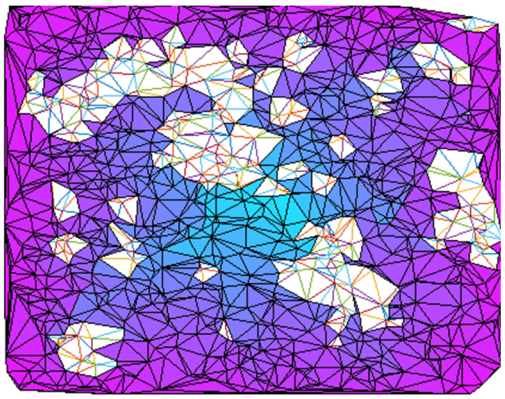

Fig. 2. Deleting the undesired simplexes from the design space. The feasible response can be inside the white simplexes.

Fig. 2 demonstrates that the algorithm iteratively shrinks the primary design space to find an appropriate stabilizer point for the system. In each iteration, it checks the stability situation of each corner point of the generated simplexes. Hence, it is needed to employ a condition to evaluate whether a sample design point is able to stabilize the system or not. In the following, theorem 2 is given for checking the stability condition of a sample point in the design space.

Theorem 2. *The given design point $F = [K_P \quad K_I]^T$ stabilizes the LFC system if and only if $\hat{q}(s,F,\alpha,z) = P(s,F,\alpha) + W(s,F,\alpha)z$ does not have any root whose real part is positive and its imaginary part is larger than $\frac{\arg(z)}{\bar{\tau}}$ for $\alpha \in \Omega$ and z on the boundary of the unit circle in the complex plane.*

Proof. It is apparent that the existence of a root with positive real part un-stabilizes the closed loop system. Thus, it suffices to prove the stability of the system under the condition that the root imaginary part is larger than $\frac{\arg(z)}{\bar{\tau}}$. It is clear that $\hat{q}(s,F,\alpha,z)$ equals to $q(s,F,\alpha,\tau)$ considering $z = e^{-\tau s}$ that means the characteristic polynomial $q(s,F,\alpha,\tau)$ does not have any root in the Right Half Plane (RHP) part of the complex plane for all $\alpha \in \Omega$ and $\tau \in [0,\bar{\tau}]$. If $\tau\omega > \arg(z)$, the condition is not satisfied. This fact implies the closed loop system is stable for the pre-considered given design point F.□

Remark 2. *It is notable that the considered design point stabilizes the closed loop system if and only if the assumptions of Theorem 2 are satisfied. This means that Theorem 2 is an*

equivalent theorem, while Theorem 1 was not an equivalent one and imposes some conservativeness.

Remark 3. *It is worth mentioning that the conditions of Theorem 2 cannot be evaluated by the common solving algorithms due to their nonlinearities and non-convexities. It is mainly because it must be checked that whether polynomial $\hat{q}(s,F,\alpha,z)$ has any roots in the specific region for all $\alpha \in \Omega$ and unit value complex number z.*

To cope with the nonlinearity of the condition of Theorem 2, the exposed edges theorem [34] is exploited which is fully explained in Theorem 3

Theorem 3. *The given design point $F = [K_P \quad K_I]^T$ stabilizes the LFC system if and only if $\hat{q}(s,F,\alpha,z) = P(s,F,\alpha) + W(s,F,\alpha)z$ does not have any root with positive real part whose imaginary part is larger than $\frac{\arg(z)}{\bar{\tau}}$ for z on the boundary of unit circle and α on the exposed edges of Ω.*

Proof. Polynomial $\hat{q}(s,F,\alpha,z)$ affinely depends on the uncertain parameters α. Due to this fact and the exposed edges theorem, boundary of the roots of a parametric polynomial such as $\hat{q}(s,F,\alpha,z)$ belongs to the roots of the exposed edges of the uncertain space which is Ω for $\hat{q}(s,F,\alpha,z)$. It is apparent that the parametric polynomial $\hat{q}(s,F,\alpha,z)$ has no root inside the specific region of the theorem for all $\alpha \in \Omega$ once it has no root at the exposed edges of the uncertain space.

Theorem 3 states that the given design point F stabilizes the LFC system if polynomial $\hat{q}(s,F,\alpha,z)$ does not have any non-Hurwitz root whose imaginary part is larger than $\frac{\arg(z)}{\bar{\tau}}$ for α on the exposed edges of the uncertain space which are the edges of the Ω .

Paper [35] develops a factual methodology to assess the existence of a root inside any compact region of the complex plane for a given line segment between two particular points of the design space. This methodology enables us to assess the conditions of Theorem 3 through an appropriate algorithm.

C. *Direct search-based algorithm*

The original direct search algorithm [35] is applicable for stability analysis with any number of controller design parameters, and it is adopted for the LFC system of Section II. Since the PI controller of the LFC comprises two gains K_p and K_I, the design space is turned into a two-dimensional triangular space, as shown in Fig. 3(a). To check a feasible solution Fig. 3(a), we start with checking the stability of the corner points based on the idea of the previous subsection, as shown in Fig 3(b). For each of these points, one has a solution vector $F_i = [K_{pi} \quad K_{Ii}]$ for $i = 1,2,3$ that should be obtained by evaluating these corner points in $\hat{q}(s,F,\alpha,z)$ defined in Theorem 3. Then, three polynomials are obtained that should be checked to have any inappropriate root in terms of the assumptions of Theorem 3, as follows.

$$\hat{q}_i(s,F_i,\alpha,z) \text{ for } i = 1,2,3 \qquad (26)$$

For the admissible ranges of T and α, the stability of polynomial $\hat{q}_i(s,F_i,\alpha,z)$ should be checked [36]. This stage is called checking method 1 (CM1). The CM1 can be done by checking the polynomial roots. If all of its roots have negative real values, the polynomial and its corresponding closed-loop system are stable. If for any of the points F_i, the roots of $\hat{q}_i(s,F_i,\alpha,z) = 0$ have negative real parts, that point is a feasible solution and the controller is designed. Otherwise, we need to proceed with the direct search algorithm.

In the next step, we are sure that the corner polynomials are infeasible and none of them can stabilize the characteristic polynomial of the closed loop system. We want to check whether the whole simplex is infeasible or there may be a feasible solution inside the simplex. For this aim, the stability of the edges of the triangular space should be checked. Since the places of the corner points are known, it is a simple task to find the representation of the edges. The edge or line segment representation can be obtained by the convex combination of its corresponding corner points F_i and F_j, using (27).

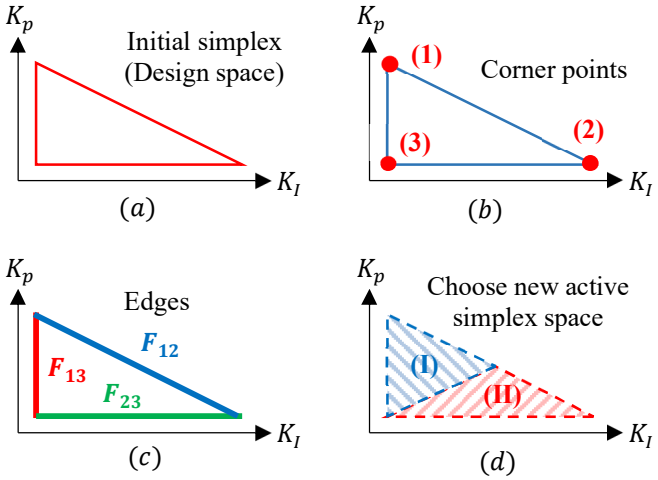

Fig. 3. Each step of the direct search iteration algorithm.

$$F_{ij} = \gamma F_i + (1-\gamma)F_j \text{ for } i < j = 1,2,3 \text{ and } 0 \le \gamma \le 1 \qquad (27)$$

As can be seen in Fig. 3(c), for each edge F_{ij} for $i < j = 1,2,3$, three sets of polynomials with respect to the γ value are obtained, as follows:

$$\hat{q}_{ij}(s,F_{ij},\alpha,z,\gamma) \text{ for } i < j = 1,2,3 \qquad (28)$$

Now the stability of polynomials (28) is checked. This step is called checking method 2 (CM2). If none of the polynomials in (28) have pure imaginary roots, then the whole simplex is infeasible and we cannot find any solution to the problem [37]. Otherwise, there may still be a feasible solution in the active simplex. In this step, the current simplex is halved with respect to its largest edge, as shown in Fig. 3(d). Then, for one of the randomly selected sub-simplexes (i.e. (I) or (II)), the new active simplex space is chosen and the net integration is performed. If a feasible solution cannot be found in the active simplex (for instance, i.e. (I) in Fig (3d)), then the other apace will be checked (for instance, i.e. (II)) and the algorithm continues.

The details of the steps CM1 and CM2 and the convergence proof can be found in [35]. The overall iterative algorithm is given in Fig. 4. It should also be noted that the algorithm shrinks the triangles till their areas are larger than a prespecified threshold denoted by δ. Fig. 4 demonstrates the step-by-step theoretical method needed for designing the controller. It should be noted that by employing our proposed approach, the overall controller is of a PI type and it can be easily implemented in practice.

D. *Performances of the proposed algorithm*

The proposed algorithm has some advantages that are discussed in this subsection. It will be shown that the algorithm has finite number of iterations and it converges to a feasible solution inside the primary design triangle under some slight conditions. These advantages are separately presented in the sequel.

Theorem 4. *Direct search-based algorithm will terminate in* $\frac{v_0}{\delta}$ *in which* v_0 *is the area of the primary design triangle.*

Proof. Notice that, the algorithm continues until there exists a triangle whose area is larger than δ which is a given threshold over the areas of the tringles. Through this mechanism, it is clear that the algorithm will surely stop once there is no acceptable triangles to be checked. It means the number of the algorithm's iterations cannot exceed $\frac{v_0}{\delta}$ based on the mentioned fact.

Theorem 5. *The proposed algorithm reaches a stabilizer point whenever there exists a feasible region inside the primary design triangle whose area is larger than* δ.

Proof. Based on the steps of the algorithm, it checks the corner points of all generated triangles till it finds a feasible solution or there is not any acceptable triangle to be checked. Since, it has been supposed that there exists a feasible region whose area is larger than δ, the algorithm will surely reach a triangle that its intersection with the premised feasible region is not empty. Hence, the algorithm surely finds a feasible point inside the mentioned feasible region in one of its iterations.

Theorems 4 and 5 prove that the algorithm terminates in a finite number of iterations and converges into a feasible region if it exists. The algorithm finitely converges a feasible solution once there is a feasible region with a suitable area.

IV. Simulation Results

In this section, the closed-loop stability of the LFC system is evaluated and the effect of system uncertainties and time delay value on the stability in the $(K_p\ , K_I)$-plane is investigated. Also, the PI controller gain regions for which the closed-loop system is stable will be obtained. Finally, validation studies employing time-domain simulations are given.

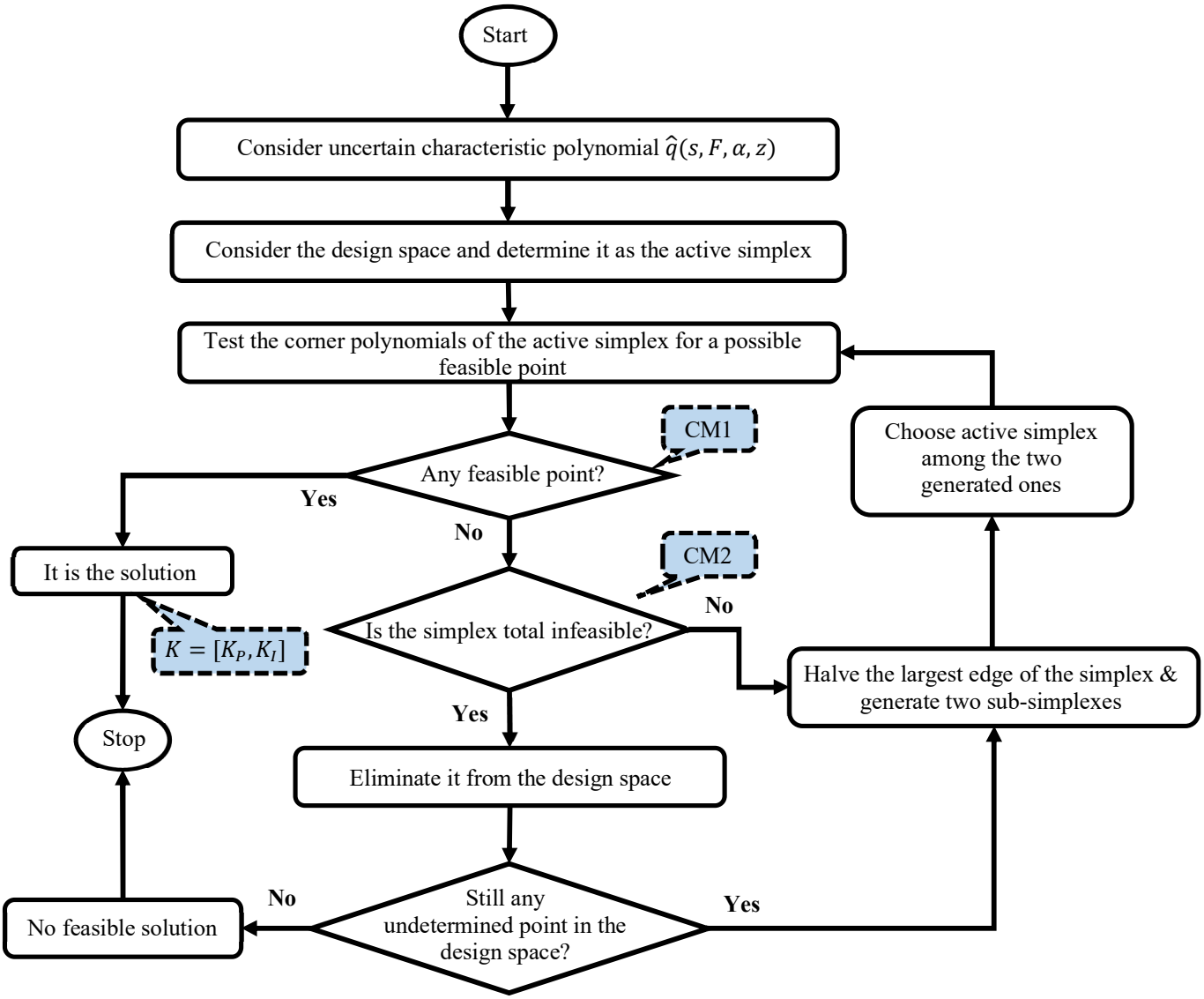

Fig. 4. The flowchart of the overall algorithm.

A. Scenario 1 (Effect of system uncertainties on the stability region)

In this scenario, to show the impact of the system uncertainties on the closed-loop stability, the time delay values are fixed by $\tau = 0.5$ and 1 and two ranges for the participation factors α_0 and α_1 are considered as shown in Table II. Deploying the direct search and Lyapunov Krasovskii based algorithm, Figs. 5 and 6 are obtained. Indeed, these figures are provided to compare the ability of these algorithms to stabilize the LFC power system. In these figures, the blue and magenta regions show the feasible regions of the direct search and LKF-based algorithms, respectively.

As can be seen in Figs. 5 and 6, by approaching the range of α_0 to one and α_1 to zero, the stability region is enlarged because when α_1 tends to zero, the effect of EV aggregator with delay term is decreased. This relaxes the stability analysis and eases finding a feasible solution. So, a larger stability range is obtained. Also, the regions of Figs. 5(a) and 6(a) are a subregion of those in Figs. 5(b) and 6(b), respectively.

Figs. 5 and 6 also show the feasible regions of the LKF-based algorithm. As can be seen from them, the feasible regions of this algorithm fully belong to the feasible regions of the direct search-based algorithm. This means that the direct search-based algorithm can stabilize the LFC power system better than Lyapunov Krasovskii based one. This result is formerly confirmed by Theorem 5, which shows that the direct search algorithm is able to find a feasible solution once a slight condition is satisfied; however, this phenomenon cannot be generally guaranteed by the Lyapunov Krasovskii algorithm.

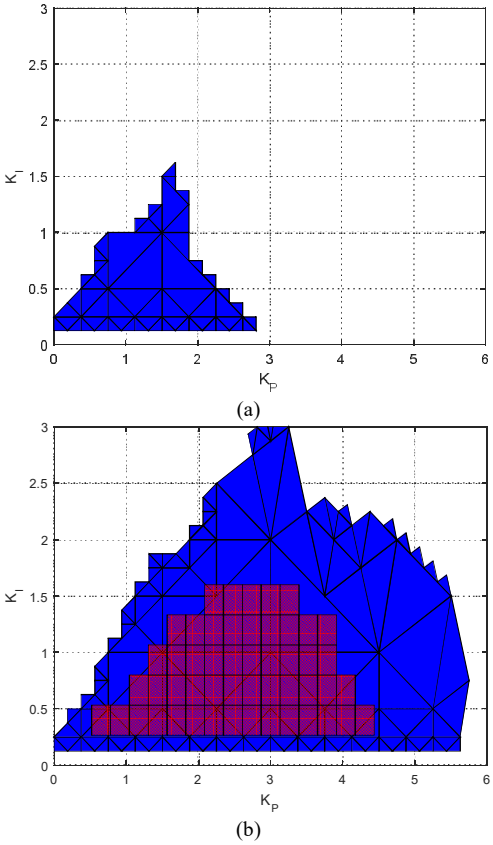

Fig. 5. Stability regions for $\boldsymbol{\tau = 0.5}$: (a). $\boldsymbol{\alpha_0 = [0.7, 1]}$, $\boldsymbol{\alpha_1 = [0, 0.3]}$, (b). $\boldsymbol{\alpha_0 = [0.9, 1]}$, $\boldsymbol{\alpha_1 = [0, 0.1]}$.

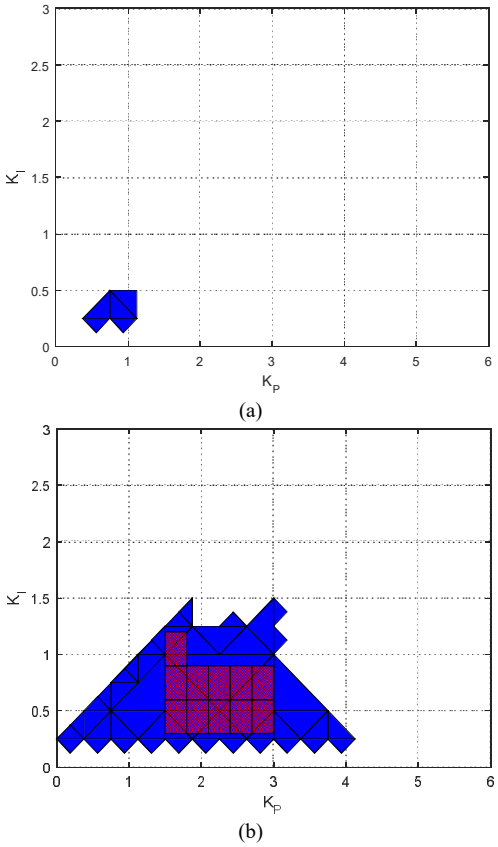

Fig. 6. Stability regions for $\boldsymbol{\tau = 1}$: (a). $\boldsymbol{\alpha_0 = [0.7, 1]}$, $\boldsymbol{\alpha_1 = [0, 0.3]}$, (b). $\boldsymbol{\alpha_0 = [0.9, 1]}$, $\boldsymbol{\alpha_1 = [0, 0.1]}$.

TABLE II. THE PARAMETERS OF LFC SYSTEM IN SCENARIO 1.

Figure number	τ	α_0	α_1
5(a)	0.5 s	[0.7,1]	[0,0.3]
5(b)	0.5 s	[0.9,1]	[0,0.1]
6(a)	1 s	[0.7,1]	[0,0.3]
6(b)	1 s	[0.9,1]	[0,0.1]

It should be emphasized that the LKF-based algorithm does not find any feasible solution for the uncertain case $\Omega = [0.7,1] \times [0,0.3]$. It means that the feasibility performance of this algorithm depends on the size of the uncertain space, which is another drawback of this algorithm. Notice that, the other parameters in these simulations are supposed to be the same, except the size of the uncertain space, to be able to directly focus on the effect of system uncertainties.

B. Scenario 2 (Effect of time delay on the stability region)

In a similar manner to Scenario 1, to show the impact of the time delay on the closed-loop stability, in this scenario, the system uncertainty range is fixed by $\alpha_0 = [0.9,1]$ and $\alpha_1 = [0,0.1]$. On the other hand, two values for the time delay are chosen as $\tau = 0.5$ and $\tau = 1.5$, as summarized in Table III.

Utilizing the direct search algorithm of Section III, Fig. 7 is achieved which reveals that the time delay adversely affects the stability region. Although the obtained region for $\tau = 1.5$ is smaller than that of $\tau = 0.5$, Fig. 7(a) is not a subset of Fig. 7(b). This can be inferred that the time delay affects the stability region nonlinearly, which is also evident from (1).

This article has been accepted for publication in IEEE Transactions on Industry Applications. This is the author's version which has not been fully edited and content may change prior to final publication. Citation information: DOI 10.1109/TIA.2022.3230018

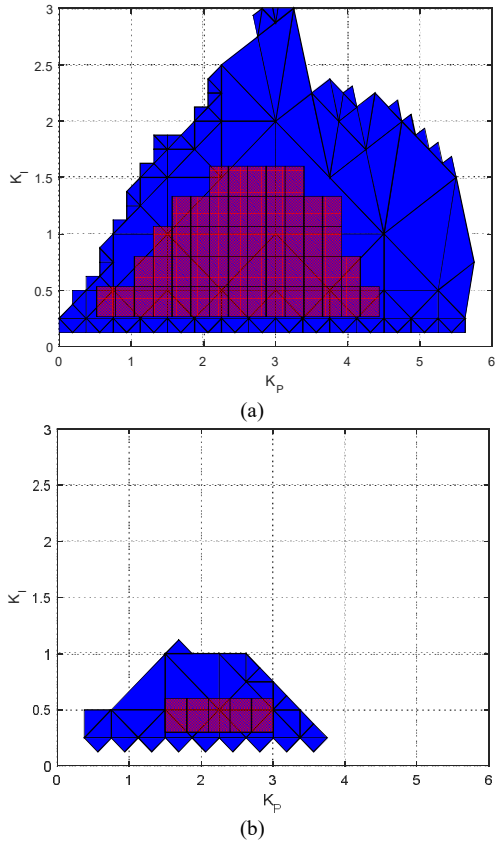

Fig. 7. Stability regions for EV aggregator participation factors $\boldsymbol{\alpha_0} = [\mathbf{0.9}, \mathbf{1}]$, $\boldsymbol{\alpha_1} = [\mathbf{0}, \mathbf{0.1}]$, (a). $\boldsymbol{\tau} = \mathbf{0.5}$, (b) $\boldsymbol{\tau} = \mathbf{1.5}$.

TABLE III. THE PARAMETERS OF LFC SYSTEM IN SCENARIO 2.

Figure number	τ	α_0	α_1
7(a)	0.5 s	[0.9,1]	[0,0.1]
7(b)	1.5 s	[0.9,1]	[0,0.1]

Based on Fig. 7, the direct search algorithm is more able to stabilize the EV aggregator over the Lyapunov Krasovskii based algorithm for the special case $\tau = 1.5$. It is another numerical evidence for the better feasibility performance of the direct search algorithm that is previously assured by the convergence analysis of the algorithm.

C. Scenario 3 (Effect of both uncertainty and time delay compared to the state-of-the-art approaches)

In this scenario, the impact of both uncertainty and time delay on the stability region of the closed loop system is compared to two state-of-the-art approaches presented in [38] and [39]. Considering the EV aggregator participation factors (parameter uncertainties) $\alpha_0 = [0.9,1]$, $\alpha_1 = [0,0.1]$, and the upper bound of time delay as $\tau = 0.8$, as it is clear from Fig. 8 and Fig. 9, the stability region of closed loop system obtained by the direct search algorithm (blue stability region) has been compared with the other previous methods (purple stability spaces). Based on Fig. 8 and 9, the direct search algorithm is capable to find a larger stability region for the EV aggregator than Method 1 and method 2. According to these figures, the two previous methods have the same stability region because most of the Lyapunov-based methods are less sensitive to the delay and more sensitive to its derivative.

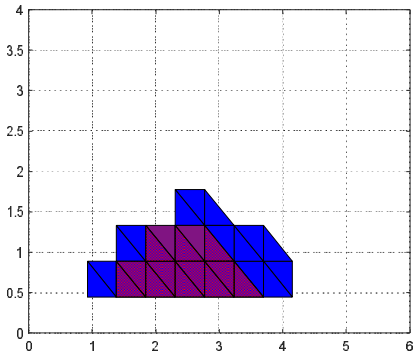

Fig. 8. Comparison of the stability regions of the proposed method and the Method 1 in [38] with parameter uncertainty $\boldsymbol{\alpha_0} = [\mathbf{0.9}, \mathbf{1}]$, $\boldsymbol{\alpha_1} = [\mathbf{0}, \mathbf{0.1}]$, and upper bound of delay $\boldsymbol{\tau} = \mathbf{0.8}$.

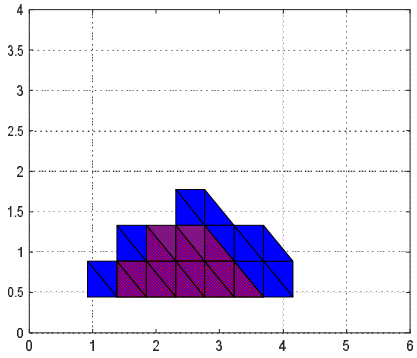

Fig. 9. Comparison of the stability regions of the proposed method and the Method 2 in [39] with parameter uncertainty $\boldsymbol{\alpha_0} = [\mathbf{0.9}, \mathbf{1}]$, $\boldsymbol{\alpha_1} = [\mathbf{0}, \mathbf{0.1}]$, and upper bound of delay $\boldsymbol{\tau} = \mathbf{0.8}$.

The computational burden of the proposed method and these two state-of-the-art approaches with upper bound of time delay $\tau_1 = 0.2$, $\tau_2 = 0.4$, $\tau_3 = 0.8$, in the presence of corners of uncertainty $\alpha_0 = [0.9,1]$, $\alpha_1 = [0,0.1]$, are compared in Fig. 10. According to Fig. 10, it is clear that, the computational burden of the direct search method is less than the other methods. The proposed algorithm is able to find a stabilizer point for the mentioned system equivalently; however, the existing LKF-based methods do not guarantee the equivalent feasibility situation since they convert the non-convex control design problem into a convex problem with a set of LMI conditions which is certainly not equivalent to the original problem. Therefore, taking both factors (conservativeness and computational burden) into account, the direct search algorithm is more beneficial in finding the design parameters.

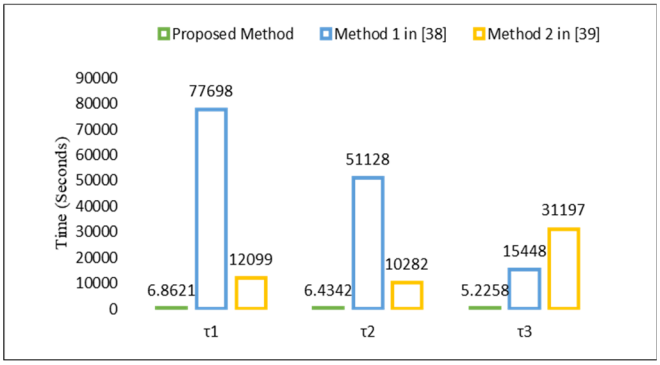

Fig. 10. Comparison of the computational burden of the proposed method with two other methods.

This article has been accepted for publication in IEEE Transactions on Industry Applications. This is the author's version which has not been fully edited and content may change prior to final publication. Citation information: DOI 10.1109/TIA.2022.3230018

D. Scenario 4 (Time-domain closed-loop model simulation)

To show the effectiveness of the proposed approach, for selected PI controller gain $K_P = 1.5, K_I = 0.5$ from Fig. 7(b) which illustrates the stability region with upper bound of time delay $\tau = 1.5$ in the presence of uncertainty $\alpha_0 = [0.9,1]$, $\alpha_1 = [0,0.1]$, the closed-loop model input and system output evolutions are provided. The load power variation is set as $\Delta P_d = 0.2$. Fig. 11 shows that the system is robust against load power changes and a time-delayed EV aggregator. Considering the PI controller $K_P = 2, K_I = 0.8$ based on the results obtained in Fig. 7(b), the effects of variable time delay with upper bound $\tau = 1.5$ and the different disturbances on the Electric Vehicle Aggregator are evaluated and the results are shown in Fig. 12.

Table IV demonstrates norms 2 and ∞ of the system output and the designed control input in presence of various disturbances. The conclusion that can be drawn from Table IV is that, considering the random disturbance, the norm 2 of the control signal is bigger than the norms of the other assessed disturbances, indicating that the control signal has made more effort to stabilize the system output. In addition, the variation of the sinusoidal disturbance compared to zero is more than those of the other disturbances leading to a higher norm 2 of system output compared to other cases.

TABLE IV. OUTPUT SYSTEM PERFORMANCE IN PRESENCE OF VARIOUS DISTURBANCES

Types	Disturbances	$\|y\|_\infty$	$\|y\|_2$	$\|u\|_\infty$	$\|u\|_2$
1	Step	0.0222	0.1143	1.0025	7.8943
2	Sinusoidal	0.0236	0.8060	1.4126	6.6582
3	Random	0.0229	0.2208	1.3377	12.8048

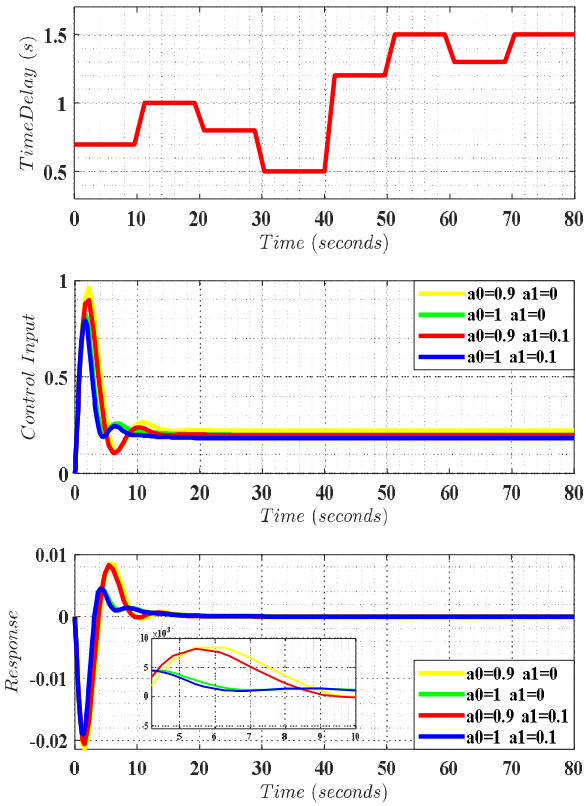

Fig. 11. The closed-loop system simulation of Scenario 3. (a). Time Delay variation, (b). Control input, (c) System Output.

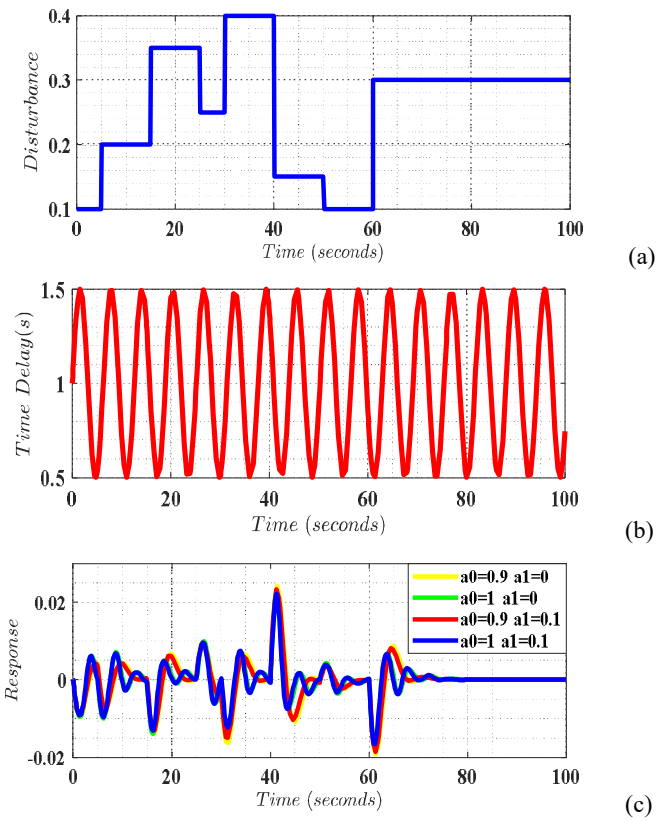

Fig. 12. The closed-loop system simulation. (a) Disturbance variation, (b). Time Delay variation, (c) System Output.

Fig. 12(c) indicates the response of the system for four corner points of the uncertainties. The EV aggregator is robust against the disturbances, uncertainties and the time delay and the frequency can be regulated.

V. Conclusion

In this paper, the challenges of connecting an EV aggregator to a single-area LFC system with non-ideal delay communication network were examined. The polynomial characteristic equation of the closed-loop system controlled by a PI controller was obtained. Then, a numerical iterative direct search algorithm was provided to determine a feasible solution for the controller gains that assure the robust closed-loop stability against system uncertainties. Several scenarios were considered to show the impact of time delay and uncertainties in EV aggregator parameters on single-area LFC stability and frequency response. It was proven and shown by simulations that the direct search algorithm is able to find the stability region in presence of uncertainties and delay, equivalently. Briefly, this approach is useful in finding infeasible points inside the design space that should be omitted instantly and discovering the feasible ones, which can stabilize the system in presence of uncertainty and time delay. For future work, considering optimal controller design for the EV aggregator is suggested.

References

[1] K. T. Farsani *et al.*, "Improved Load Frequency Control of Time-Delayed Electric Vehicle Aggregators via Direct Search Method," *Conf. Rec. - IAS Annu. Meet. IEEE Ind. Appl. Soc.*, vol. 2021-October, 2021, doi: 10.1109/IAS48185.2021.9677201.

[2] K. Torabi-Farsani, M. H. Asemani, F. Badfar, N. Vafamand, and M. H. Khooban, "Robust Mixed μ -Synthesis Frequency Regulation in AC Mobile Power Grids," *IEEE Trans. Transp. Electrification*, vol. 5, no. 4, pp. 1182–1189, Dec. 2019, doi: 10.1109/TTE.2019.2960637.

[3] A. Naveed, S. Sonmez, and S. Ayasun, "Impact of Electric Vehicle Aggregator with Communication Time Delay on Stability Regions and Stability Delay Margins in Load Frequency Control System," *J. Mod. Power Syst. Clean Energy*, vol. 9, no. 3, pp. 595–601, May 2021, doi: 10.35833/MPCE.2019.000244.

[4] A. M. Carreiro, H. M. Jorge, and C. H. Antunes, "Energy management systems aggregators: A literature survey," *Renew. Sustain. Energy Rev.*, vol. 73, pp. 1160–1172, Jun. 2017, doi: 10.1016/J.RSER.2017.01.179.

[5] K. S. Ko and D. K. Sung, "The effect of EV aggregators with time-varying delays on the stability of a load frequency control system," *IEEE Trans. Power Syst.*, vol. 33, no. 1, pp. 669–680, 2018, doi: 10.1109/TPWRS.2017.2690915.

[6] K. T. Farsani *et al.*, "Direct Search-based Delay Attack Mitigation in Electric Vehicle Aggregators," in *2021 IEEE International Conference on Environment and Electrical Engineering and 2021 IEEE Industrial and Commercial Power Systems Europe (EEEIC / I&CPS Europe)*, Bari, Italy, Sep. 2021, pp. 1–5. doi: 10.1109/EEEIC/ICPSEurope51590.2021.9584690.

[7] R. Abolpour, M. Dehghani, and H. A. Talebi, "Stability analysis of systems with time-varying delays using overlapped switching Lyapunov Krasovskii functional," *J. Frankl. Inst.*, vol. 357, no. 15, pp. 10844–10860, Oct. 2020, doi: 10.1016/J.JFRANKLIN.2020.08.018.

[8] C. Hua and Y. Wang, "Delay-Dependent Stability for Load Frequency Control System via Linear Operator Inequality," *IEEE Trans. Cybern.*, 2020, doi: 10.1109/TCYB.2020.3037113.

[9] X. Shang-Guan, Y. He, C. Zhang, L. Jiang, J. W. Spencer, and M. Wu, "Sampled-data based discrete and fast load frequency control for power systems with wind power," *Appl. Energy*, vol. 259, p. 114202, Feb. 2020, doi: 10.1016/J.APENERGY.2019.114202.

[10] H. Luo and Z. Hu, "Stability Analysis of Sampled-Data Load Frequency Control Systems with Multiple Delays," *IEEE Trans. Control Syst. Technol.*, vol. 30, no. 1, pp. 434–442, Jan. 2022, doi: 10.1109/TCST.2021.3061556.

[11] J. Li, T. Yu, and H. Cui, "A multi-agent deep reinforcement learning-based 'Octopus' cooperative load frequency control for an interconnected grid with various renewable units," *Sustain. Energy Technol. Assess.*, vol. 51, p. 101899, Jun. 2022, doi: 10.1016/J.SETA.2021.101899.

[12] T. Masuta and A. Yokoyama, "Supplementary load frequency control by use of a number of both electric vehicles and heat pump water heaters," *IEEE Trans. Smart Grid*, vol. 3, no. 3, pp. 1253–1262, 2012, doi: 10.1109/TSG.2012.2194746.

[13] A. E. Onyeka, Y. Xing-Gang, Z. Mao, B. Jiang, and Q. Zhang, "Robust decentralised load frequency control for interconnected time delay power systems using sliding mode techniques," *IET Control Theory Appl.*, vol. 14, no. 3, pp. 470–480, Feb. 2020, doi: 10.1049/IET-CTA.2019.0809/CITE/REFWORKS.

[14] E. Tian and C. Peng, "Memory-Based Event-Triggering H∞Load Frequency Control for Power Systems under Deception Attacks," *IEEE Trans. Cybern.*, vol. 50, no. 11, pp. 4610–4618, Nov. 2020, doi: 10.1109/TCYB.2020.2972384.

[15] X. C. Shangguan, Y. He, C. K. Zhang, L. Jiang, and M. Wu, "Load frequency control of time-delayed power system based on event-triggered communication scheme," *Appl. Energy*, vol. 308, p. 118294, Feb. 2022, doi: 10.1016/J.APENERGY.2021.118294.

[16] D. Wang, F. Chen, B. Meng, X. Hu, and J. Wang, "Event-based secure H∞ load frequency control for delayed power systems subject to deception attacks," *Appl. Math. Comput.*, vol. 394, p. 125788, Apr. 2021, doi: 10.1016/J.AMC.2020.125788.

[17] M. Khan, H. Sun, Y. Xiang, and D. Shi, "Electric vehicles participation in load frequency control based on mixed H2/H∞," *Int. J. Electr. Power Energy Syst.*, vol. 125, p. 106420, Feb. 2021, doi: 10.1016/J.IJEPES.2020.106420.

[18] M. H. Khooban, T. Niknam, M. Shasadeghi, T. Dragicevic, and F. Blaabjerg, "Load Frequency Control in Microgrids Based on a Stochastic Noninteger Controller," *IEEE Trans. Sustain. Energy*, vol. 9, no. 2, pp. 853–861, Apr. 2018, doi: 10.1109/TSTE.2017.2763607.

[19] F. Zhu, X. Zhou, Y. Zhang, D. Xu, and J. Fu, "A load frequency control strategy based on disturbance reconstruction for multi-area interconnected power system with hybrid energy storage system," *Energy Rep.*, vol. 7, pp. 8849–8857, Nov. 2021, doi: 10.1016/J.EGYR.2021.09.029.

[20] M. H. Khooban, "Secondary Load Frequency Control of Time-Delay Stand-Alone Microgrids with Electric Vehicles," *IEEE Trans. Ind. Electron.*, vol. 65, no. 9, pp. 7416–7422, Sep. 2018, doi: 10.1109/TIE.2017.2784385.

[21] J. Guo, "The Load Frequency Control by Adaptive High Order Sliding Mode Control Strategy," *IEEE Access*, 2022, doi: 10.1109/ACCESS.2022.3152259.

[22] T. N. Pham, H. Trinh, and L. Van Hien, "Load frequency control of power systems with electric vehicles and diverse transmission links using distributed functional observers," *IEEE Trans. Smart Grid*, vol. 7, no. 1, pp. 238–252, Jan. 2016, doi: 10.1109/TSG.2015.2449877.

[23] C. K. Zhang, L. Jiang, Q. H. Wu, Y. He, and M. Wu, "Delay-dependent robust load frequency control for time delay power systems," *IEEE Trans. Power Syst.*, vol. 28, no. 3, pp. 2192–2201, 2013, doi: 10.1109/TPWRS.2012.2228281.

[24] N. Vafamand, M. H. Khooban, T. Dragicevic, J. Boudjadar, and M. H. Asemani, "Time-Delayed Stabilizing Secondary Load Frequency Control of Shipboard Microgrids," *IEEE Syst. J.*, vol. 13, no. 3, pp. 3233–3241, 2019, doi: 10.1109/JSYST.2019.2892528.

[25] S. J. Zhou, H. B. Zeng, and H. Q. Xiao, "Load Frequency Stability Analysis of Time-Delayed Multi-Area Power Systems with EV Aggregators Based on Bessel-Legendre Inequality and Model Reconstruction Technique," *IEEE Access*, vol. 8, pp. 99948–99955, 2020, doi: 10.1109/ACCESS.2020.2997002.

[26] A. Khalil and A. S. Peng, "Delay margin computation for load frequency control system with plug-in electric vehicles," *Int. J. Power Energy Syst.*, vol. 38, no. 3, pp. 115–131, Mar. 2018, doi: 10.2316/JOURNAL.203.2018.3.203-0060.

[27] M. Ahmed, G. Magdy, M. Khamies, and S. Kamel, "Modified TID controller for load frequency control of a two-area interconnected diverse-unit power system," *Int. J. Electr. Power Energy Syst.*, vol. 135, p. 107528, Feb. 2022, doi: 10.1016/J.IJEPES.2021.107528.

[28] M. D. Galus, S. Koch, and G. Andersson, "Provision of load frequency control by PHEVs, controllable loads, and a cogeneration unit," *IEEE Trans. Ind. Electron.*, vol. 58, no. 10, pp. 4568–4582, Oct. 2011, doi: 10.1109/TIE.2011.2107715.

[29] Y. Jia, Z. Y. Dong, C. Sun, and K. Meng, "Cooperation-Based Distributed Economic MPC for Economic Load Dispatch and Load Frequency Control of Interconnected Power Systems," *IEEE Trans. Power Syst.*, vol. 34, no. 5, pp. 3964–3966, 2019, doi: 10.1109/TPWRS.2019.2917632.

[30] H. Chen, R. Ye, X. Wang, and R. Lu, "Cooperative Control of Power System Load and Frequency by Using Differential Games," *IEEE Trans. Control Syst. Technol.*, vol. 23, no. 3, pp. 882–897, May 2015, doi: 10.1109/TCST.2014.2346996.

[31] H. B. Zeng, S. J. Zhou, X. M. Zhang, and W. Wang, "Delay-Dependent Stability Analysis of Load Frequency Control Systems With Electric Vehicles," *IEEE Trans. Cybern.*, 2022, doi: 10.1109/TCYB.2022.3140463.

[32] S. Sönmez and S. Ayasun, "Stability Region in the Parameter Space of PI Controller for a Single-Area Load Frequency Control System With Time Delay," *IEEE Trans. Power Syst.*, vol. 31, no. 1, pp. 829–830, Jan. 2016, doi: 10.1109/TPWRS.2015.2412678.

[33] W. Qian, M. Yuan, L. Wang, X. Bu, and J. Yang, "Stabilization of systems with interval time-varying delay based on delay decomposing approach," *ISA Trans.*, vol. 70, pp. 1–6, Sep. 2017, doi: 10.1016/J.ISATRA.2017.05.017.

[34] B. Aguirre-Hernández, F. R. Garciá-Sosa, C. A. Loredo-Villalobos, R. Villafuerte-Segura, and E. Campos-Cantón, "Open Problems Related to the Hurwitz Stability of Polynomials Segments," *Math. Probl. Eng.*, vol. 2018, 2018, doi: 10.1155/2018/2075903.

[35] R. Abolpour, M. Dehghani, and H. A. Talebi, "Output feedback controller for polytopic systems exploiting the direct searching of the design space," *Int. J. Robust Nonlinear Control*, vol. 29, no. 15, pp. 5164–5177, Oct. 2019, doi: 10.1002/RNC.4673.

[36] V. L. Kharitonov, S. I. Niculescu, J. Moreno, and W. Michiels, "Static output feedback stabilization: Necessary conditions for multiple delay controllers," *IEEE Trans. Autom. Control*, vol. 50, no. 1, pp. 82–86, Jan. 2005, doi: 10.1109/TAC.2004.841137.

[37] R. Abolpour, M. Dehghani, and H. A. Talebi, "A non-conservative state feedback control methodology for linear systems with state delay," *https://doi.org/10.1080/00207721.2021.1892235*, vol. 52, no. 12, pp. 2549–2563, 2021, doi: 10.1080/00207721.2021.1892235.

[38] W. I. Lee, S. Y. Lee, and P. Park, "Affine Bessel–Legendre inequality: Application to stability analysis for systems with time-varying delays," *Automatica*, vol. 93, pp. 535–539, Jul. 2018, doi: 10.1016/j.automatica.2018.03.073.

[39] H.-B. Zeng, Y. He, M. Wu, and J. She, "Free-Matrix-Based Integral Inequality for Stability Analysis of Systems With Time-Varying Delay," *IEEE Trans. Autom. Control*, vol. 60, no. 10, pp. 2768–2772, Oct. 2015, doi: 10.1109/TAC.2015.2404271.